Effect of Hole Size on the Fracture of Graphene Nanomesh

H. Y. Zhang, J. Y. Wu[a], J. Y. He[b] and Z. L. Zhang[c]

NTNU Nanomechanical Lab, Department of Structural Engineering, Norwegian University of Science and Technology (NTNU), 7491, Trondheim, Norway

[a] jianyang.wu@ntnu.no, [b] jianying.he@ntnu.no, [c] zhiliang.zhang@ntnu.no

Keywords: Graphene nanomesh, mechanical properties, fracture, molecular dynamics simulation

Abstract Graphene nanomesh, with high density arrays of holes to mimic interconnected nanoribbon networks, opens up enormous potential for applications in electronics. It has been shown in the literature that the graphene nanomesh is able to sustain two orders of magnitude larger amount of current than the individual graphene nanoribbons and the on/off ratio can be easily tuned through varying the neck width. The mechanical and fracture properties which are extremely important for the design of the nanotransistors, remains unexplored so far. In this study we symmetrically investigated the fracture properties of graphene nanomesh under uniaxial tension by molecular dynamics simulation. The effects of the graphene size and the hole diameter on the mechanical properties of graphene nanomesh have been analyzed. It has shown that the presence of holes can significantly deteriorate the fracture strength compared to the perfect graphene; however, its effect on the Young's modulus is quite limited. The ratio of the hole to system size appears not to be the factor weakening the fracture strength of the graphene nanomesh.

Introduction

Graphene, one-atom-thick planar sheet of sp^2-bonded carbon atoms that are densely packed in a honeycomb crystal lattice, possesses many superior properties, such as mechanical, thermal and electrical properties [1]-[3]. Graphene has significant potential for application in electronics, such as graphene-based field-effect transistors which have been developed quickly and considered as a candidate material for post-silicon age. But the nature of semimetal with zero bandgap prevents its applications in transistors at room temperature [4]. Graphene nanoribbons with well-defined widths and specific edges open up a band-gap that is large enough for transistor operation, but these nanoribbon devices often have low driving currents or transconductances [5]. However, a new graphene nanostructure, so-called graphene nanomesh, with high density array of nanoholes etched into graphene to mimic interconnected graphene nanoribbon networks [6]-[8], which can open a band-gap in a large sheet of graphene to create a semiconducting thin film. The Graphene nanomesh based field-effect transistors can sustain currents nearly two orders of magnitude larger than an individual graphene nanoribbon and the on-off ratio can be easily tuned by changing the neck width.

Both experimental and simulation studies have demonstrated that graphene is the strongest materials with Young's modulus of nearly 1TPa and fracture strength of more than 100GPa [9][10]. These measurements, simulations and calculations indicate that the zigzag edge graphene has much higher fracture strength and strain than the armchair one, considering that the range of the bond angle variation in zigzag edge graphene is much larger than that in armchair one, as shown in Fig. 1. However, the mechanical properties of graphene nanomesh remain unexplored. Understanding the mechanical properties of the graphene nanomesh is of great importance for their utilization in nano-electromechanical system.

zigzag direction(ZZ)   armchair direction(AM)

(a)   (b)

Fig. 1. Schematic of tension in (a) zigzag and (b) armchair direction.

In this paper, we systematically investigate the effect of nanohole size and system size on the fracture of graphene nanomesh under uniaxial tension by molecular dynamic simulation. The simulation details are described in next section. The results are analyzed in section 3, followed by the conclusions and suggestions for future work.

Methods

Molecular dynamics simulations are carried out on the fracture of graphene nanomesh using LAMMPS based on the adaptive intermolecular reactive empirical bond order (AIREBO) potential [11]. AIREBO potential is derived from a well-known dissociable hydrocarbon force field, the reactive empirical bond order (REBO) [12]. By Comparing to REBO potential, the AIREBO potential includes an adaptive treatment of non-bonded and dihedral angle interaction besides REBO term. Both potentials have been successfully employed to capture the bond breaking and bond reformation between carbon atoms for bulk carbon system. By simulating the fracture of carbon nanotube or graphene without adjusting of cutoff, the initial cutoff function introduces a sharp increase of bond forces near the cutoff distances, which causes spurious increase in fracture stress and strain [13]. To explore a suitable cutoff to overcome the deficiency, we have tuned the cutoff parameter from 1.7Å to 2.0Å under a tension test in zigzag direction of graphene sheet, as shown in Fig. 2. It can be observed that a sharp increase on tensile stress happens at the late stage resulting in an ultra-high fracture stress and strain occur when the cutoff parameter is below 2.0Å. The cutoff plays a critical role on the mechanical properties of graphene. A cutoff with 2.0Å is proved to describe the bond breaking and rehybridization instead of the bond reformation.

Fig. 2. Tensile stress-strain relationships of graphene with different cutoff values.

Periodic boundary conditions along the graphene basal plane have been adopted to avoid edge effects. The system, with a time-step of 0.5fs, first equilibrated in NPT ensemble at 300K for 50ps based on the Nose-Hoover thermostat. Then the deformation-control mode has been applied to implement the uniaxial tensile test, with a strain rate of 0.0005ps^{-1} along zigzag or armchair edge directions. During the deformation of graphene nanomesh, the strain is defined as

$$\varepsilon_x = \frac{\Delta l_x}{l_{x0}}, \;\; \varepsilon_y = \frac{\Delta l_y}{l_{y0}} \tag{1}$$

where Δl_x, Δl_y are the displacement of graphene along x and y direction, and l_{x0}, l_{y0} are the initial length in x and y direction, respectively. The stress tensor is calculated according to

$$\sigma_{ij}^\alpha = \frac{1}{V^\alpha}\left(\frac{1}{2}m^\alpha v_i^\alpha v_j^\alpha + \sum_{\beta=1,n} r_{\alpha\beta}^j r_{\alpha\beta}^i\right) \tag{2}$$

where i and j are the indices in coordinate system; α, β are the atomic indices; m^α and v^α are the mass and velocity of atom α; $r_{\alpha\beta}$ is the distance between the two atoms; and V^α is the atomic volume of atom α. Since the sheet interspacing in bulk graphite is 3.35Å, we adopt this value as nominal height of a single layer graphene to calculate the atomic stress.

The Young's modulus of tested nanomesh is obtained by fitting the linear elastic regime in stress-strain curves. The fracture stress and fracture strain are the corresponding values at the starting point of stress drop in stress-strain curves. In Fig. 2, it can be calculated that the Young's modulus of pristine graphene is 1TPa. The results agree very well with the experimental result of 1TPa or ab initio calculation of 1.05 TPa. Graphene is a six-fold rotational symmetry; according to continuum mechanics, such six-fold symmetry has an isotropic elastic and bending moduli in the basal plane. The fracture strength and fracture stain are around 0.21 and 109GPa in zigzag directions. It is noted that the fracture stress of graphene in both directions are underestimated. This finding is consist with the previous study on carbon nanotubes with and without defects based on REBO potential [14].

Results and discussions

In the experiments, graphene nanomesh is formed in the O_2 plasma, so oxygen can be used to terminate unsaturated carbon bond at the edge of the hole. Some studies have terminated the unsaturated carbon bond with hydrogen atoms and showed show that the termination with hydrogen has a negligible effect on the mechanical properties of bulk graphene [15]. Thus, graphene nanomesh systems without consideration of saturation of carbon atoms at the edge are considered in our work.

A series of uniaxial tensile tests of graphene nanomesh with 1 hole in different size along armchair direction(y direction) are first performed. Because of the applied periodic boundary conditions in x and y directions, the 1-hole graphene sheet can be considered as ordered array of nanomesh. To get such series of 1-hole graphene, a hexagonal ring is moved to obtain a graphene nanomesh with smallest hole, then one and one layer atoms along this hexagon hole are remove to enlarge the hole size in the graphene. According to the largest number of missing atoms in the direction normal to tensile direction, we denote the graphene nanomesh with 2, 4, 6 and so on, as shown in the inset of Fig. 3. In the experiments, graphene nanomesh is formed in the O_2 plasma, so oxygen can be used to terminate unsaturated carbon bond at the edge of the hole. Some studies have terminated the unsaturated carbon bond with hydrogen atoms and showed show that the termination with hydrogen has a negligible effect on the mechanical properties of bulk graphene [15]. Thus, graphene nanomesh systems without consideration of saturation of carbon atoms at the edge are considered in this work.
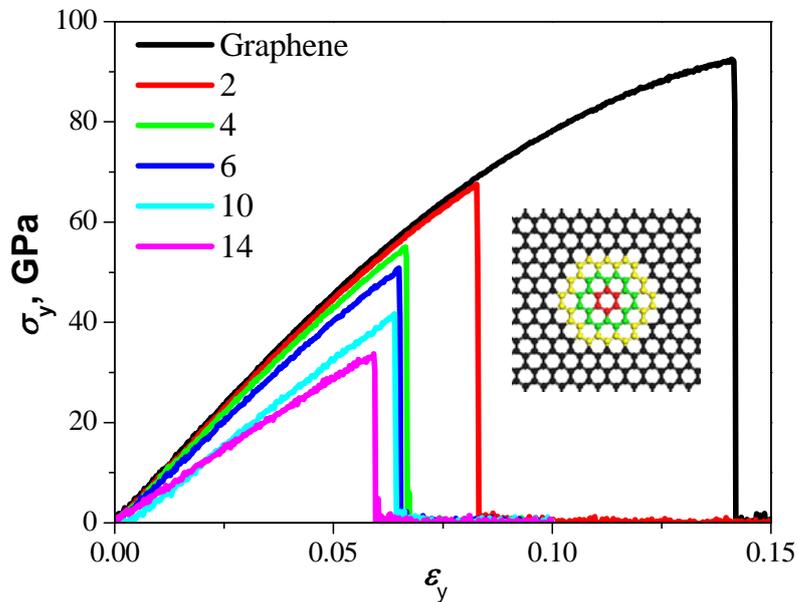
Fig. 3. Stress-strain curves and definition of hole index. The tensile direction is along armchair direction. The red, green and yellow means 1st, 2nd and 3rd ring formed.

The stress-strain curves for various hole size of nanomesh are shown in Fig. 3, compared with a pristine graphene. It can be seen that the fracture stress decreases sharply with the increase of hole size, which is consist with the previous study on carbon nanotubes [14]. In the simulation, the

system size keeps constant, therefore the neck width (defined as the smallest edge-to-edge distance between two neighboring nanoholes) decreases as the hole size increases. Because the hole size is comparable with the system size, finite-size effects are introduced. Mottoni suggests that, the finite-size effect will become significant when the ratio of system size to defect size is below 10, which can lead to the actual maximum stress at the crack tip overcoming the fracture stress before propagation [16]. In our cases, this ratio is between 14 and 1.4. We adopt the total average stress rather than the local stress at the end of graphene and then normalize the stress to the actual length in the crack plane, which is the net section stress and plotted into Fig. 4. It can be seen that the normalized fracture stress are nearly the same when the ratio is less than 10.

The net section stress is the average stress in the crack propagation plane, but the fracture is actually determined by the localized high stresses near the crack tip. To better understand the fracture, the atomic stresses at the moment of bond breaking and fracture initiation are analyzed. We first calculate the stress tensor of each atom along x or y direction. Fig. 5 shows the stress distribution along x and y directions at the time-step prior to fracture. Interestingly, only 2-3 layers of atoms are significantly influenced by the hole edges. The atoms at the edge suffer the compressive stress due to the surface effect, while the second layer of atoms are stretched. In all cases, the cracks always initiate from the bond located at the edge of the hole at which the atoms sustain the highest stresses. Because of the symmetric structure, the first bond to break may occur at either the left or right side of the hole edge. As the strain increases, crack propagates along the middle plane and the graphene separates to two parts catastrophically.
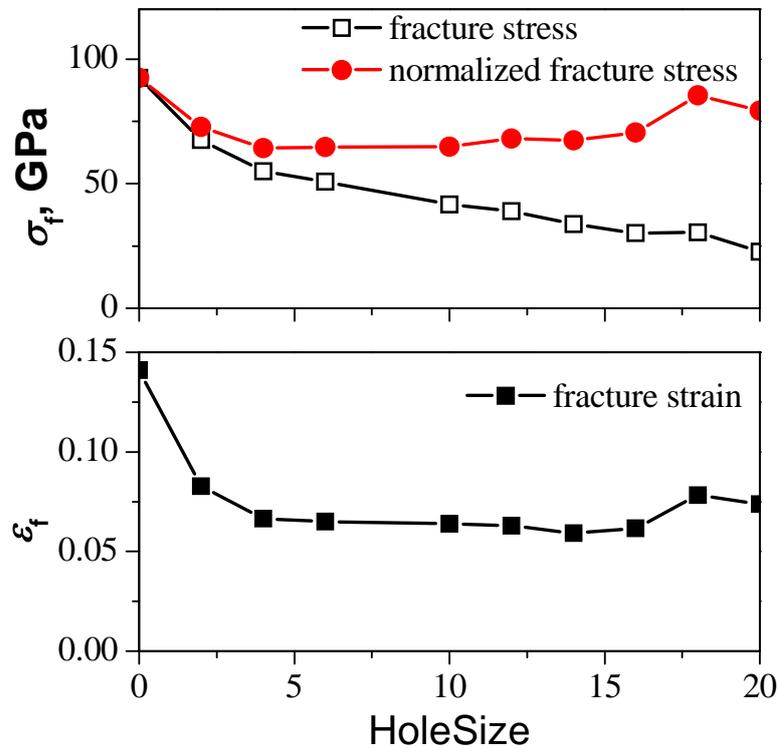
Fig. 4. Fracture stress and strain of graphene nanomesh with different hole size.
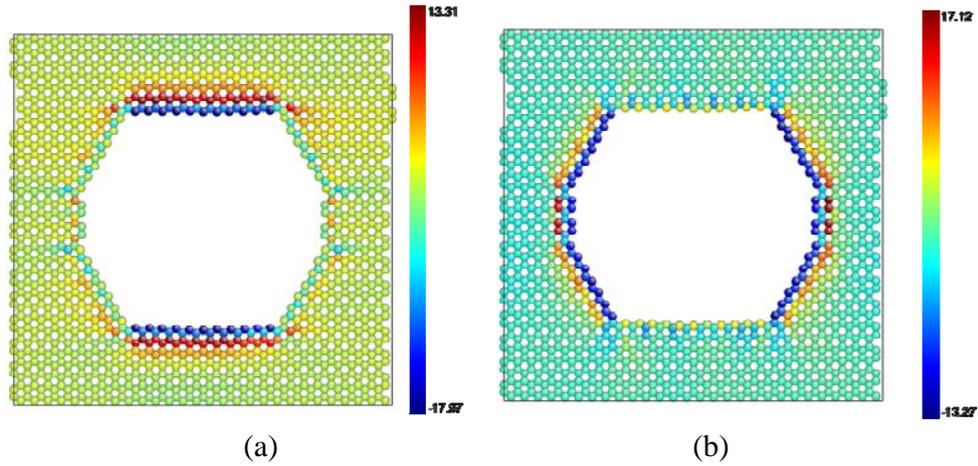
Fig. 5. Stress distribution of graphene with hole size 18 at equilibrium state: (a) stress in x direction and (b) stress in y direction. Stress unit is GPa.

In addition to the effect of the hole size, the effect of system size on the fracture properties of graphene nanomesh is also examined, as shown in Fig. 6. Compared to the initial size of 68 Å × 67.5 Å, a double system size 136 Å ×135 Å has been considered. The corresponding fracture stress and strain are summarized in Table 1. We extract fracture stress and fracture strain values from the stress-strain curve of the two different system size, shown in Table 1. From Table 1, we find that the fracture properties are independent on the system size and mainly determined by the size of involved hole.

Table 1.   The system size effect on fracture properties of graphene with 1 hole

Hole Size	Small Size		Large Size	
	σ_f	ε_f	σ_f	ε_f
Graphene	92.49317	0.140999	91.68474	0.138249
2	67.55042	0.082721	68.16589	0.08257
4	55.04896	0.066468	55.3683	0.063888
6	50.85249	0.064961	49.87908	0.058049

Similar to carbon nanotube, the fracture properties of graphene with defects are related to the effective length of defects rather than the geometry [17]. That is to say, the round holes, the hexagonal holes and slits will have the same fracture stress and fracture strain if they have the same length normal to the tensile direction. Accordingly the theory of slit is applied into hole defects. Because of the periodic boundary conditions, the graphene sheet with 1 hole can be considered as an array of slit under a remote tension, as the insert shown in Fig. 6. From the continuum mechanics point of views, the interactions between the cracks under a far-field stress of σ_∞ can be estimated using the stress intensify factor, K. If K is over a critical value, then the crack will begin to propagate. For arrays of cracks, the stress intensify factor K can be denoted with

$$K = \sigma_\infty \sqrt{(2b)tan\left(\frac{\pi a}{2b}\right)} \tag{3}$$

where $2b$ is the distance between two slits and $2a$ is the crack length. The above equation shows that, the nondimensional stress intensity factor, $K = \sigma_\infty \sqrt{a}$ is a function with b/a. When intercrack spacing $2b$ increase, the stress intensity factor should decrease because of the decrease of the interaction of the stress field. When b/a is large enough, there will be no interactions between two defects.
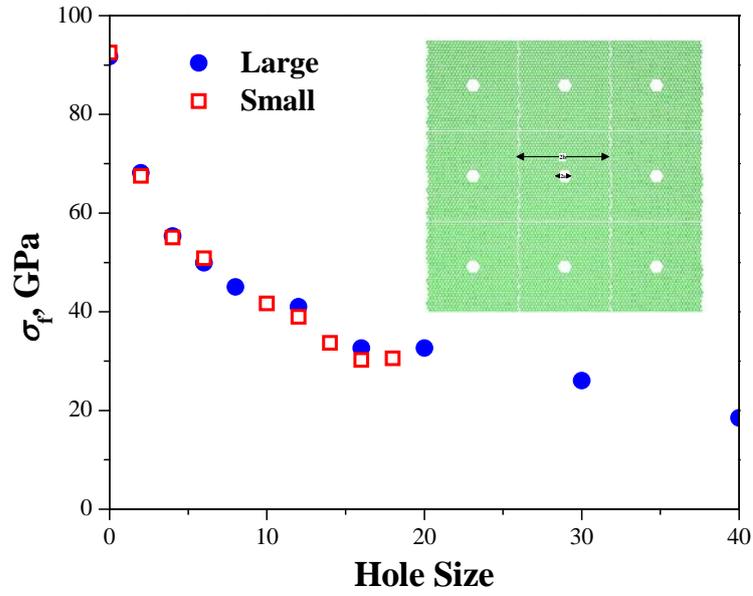
Fig. 6. System size effect on the fracture of graphene. The dimension of the small and large size is 68Å×67Å and 136Å×135Å. The inset shows the definition of $2b$ and $2a$ in arrays of holes.

Summary

The mechanical properties of graphene nanomesh have been investigated by molecular dynamic simulation. The graphene nanomesh with an array of holes is simplified to a graphene sheet with one hole in the middle by introducing periodic boundary condition. It has been found that the presence of the hole can significantly decrease the fracture strength of graphene; however, the influence on the Young's modulus is negligible. The ratio between hole size to system size appears unprevailing to the weaken effect. Instead, the absolute size of hole dominate the decrease in fracture stress and fracture strain. The increasing size of hole will significantly decrease the fracture strength of graphene nanomesh.

Acknowledgements

References

[1]   A. K.Geim: Science Vol. 324 (2009), p. 1530.

[2] A. A. Balandin: Nat. Mater. Vol. 10 (2011), p. 569.

[3] C. Lee, X. D. Wei, J. W. Kysar and J. Hone: Science Vol. 321 (2008), p. 385.

[4] F. S. Schwierz: Nat. Nanotech. Vol. 5 (2010), p. 487.

[5] Y. W.Son, M. L. Cohen and S. G. Louie: Phys. Rev. Lett. Vol. 97 (2006), p. 216803.

[6] J. W. Bai, X. Zhong, S. Jiang, Y. Huang and X. F. Duan: Nat. Nanotech. Vol. 5 (2010), p. 190.

[7] M. S. Arnold, M. K. Kim, N. S. Safron, E. Han and P. Gopalan: Nano Lett. Vol. 10 (2010), p. 1125.

[8] Y. Huang and J. B. Bai: Mat. Sci. Eng. R Vol. 70 (2010), p. 341.

[9] H. Zhao, K. Min and N. R. Aluru: Nano Letts. Vol. 9 (2009), p. 3012.

[10] Q. X. Pei, Y. W. Zhang and V. B. Shenoy: Carbon Vol. 48 (2010), p. 898.

[11] S. J. Stuart, A. B. Tutein and J. A. Harrison: J. Chem. Phys. Vol. 112 (2000), p. 6472.

[12] D. W. Brenner, O. A. Shenderova, J. A. Harrison, S. J. Stuart, B. Ni and S. B. Sinnott: J. Phys. Condens Mat. Vol. 14 (2002), p. 783.

[13] T. Belytschko, S. P. Xiao, G. C. Schatz and R. S. Ruoff: Phys. Rev. B Vol. 65 (2002), p. 235430.

[14] S. L. Mielke, D. Troya, S. Zhang, J. L. Li, S. P. Xiao, et al: Chem. Phys. Lett. Vol. 390 (2004), p. 413.

[15] C. D. Reddy, A. Ramasubramaniam, V. B. Shenoy and Y. W. Zhang: Appl. Phys. Lett. Vol. 94 (2009), p. 101904.

[16] A. Mattoni, L. Colombo and F. Cleri: Phys. Rev. Lett. Vol. 95 (2005), p.115501.

[17] S. L. Zhang, S. L. Mielke, R. Khare, D. Troya, R. S. Ruoff, et al: Phys. Rev. B Vol. 71 (2005), p. 115403.